Predictions of droplet heating and evaporation: an application to biodiesel, diesel, gasoline and blended fuels

Al Qubeissi, M

DOI 10.1016/j.applthermaleng.2018.03.010
ISSN 1359-4311
ESSN 1873-5606
Publisher: Elsevier

Predictions of droplet heating and evaporation: an application to biodiesel, diesel, gasoline and blended fuels

Mansour al Qubeissi

Centre for Mobility & Transport, Faculty of Engineering, Environment and Computing, Coventry University, Coventry, UK; email: ac1028@coventry.ac.uk

Abstract

This work is focused on the analyses of automotive fuel droplets' heating and evaporation with application to biodiesel, diesel, gasoline, and blended diesel-biodiesel fuels. The analyses are made considering conditions representative of real internal combustion engines. The evolutions of droplet radii and temperatures for gasoline, diesel, and a broad range of biodiesel fuels and their selective diesel fuel blends have been predicted using the Discrete Component model (DCM). These mixtures are combined with up to 116 components of 98 hydrocarbons and 4-18 methyl esters. The results are compared with the predictions of the case when blended biodiesel/diesel fuel are represented by pure fossil and biodiesel fuels. In contrast to previous studies, it is shown that droplet evaporation time and surface temperature predicted for 100% biodiesel are not always close to those predicted for pure diesel fuel, but they are entirely dependent on the biodiesel fuel composition. Also, the previously introduced multi-dimensional quasi-discrete model and its application to the aforementioned fuels are discussed. The application of the latter model contributes to improving the CPU efficiency with up to 96% in computational time compared to the original approach (the DCM), with a minimal loss in the accuracy of the model predictions.

Keywords

Biodiesel, Diesel, Fuel blends, Gasoline, Droplet, Heating and evaporation

1. Introduction

There have been many studies to simulate fuel droplets heating and evaporation (e.g. [1–5]); their findings have shown that modelling approaches based on the analysis of individual components, i.e. the discrete component model (DCM), produce the highest accuracy in comparison to previous approaches [6–8].

Based on recent research findings, the drawbacks in modelling fuel droplets heating and evaporation processes (computationally expensive models, ignoring temperature gradient and transient species diffusion) have been addressed using the multi-dimensional quasi-discrete model (MDQDM). In the MDQDM, a large number of components are replaced with a small number of representative components (described as 'quasi-components') [9–12]. The previous use of this model, however, has been limited to quasi-components of individual fuels, without fully considering the quasi-components of fuel blends. Also, it has been tested with a limited range of biodiesel fuel types and their mixtures with diesel fuel, rather than the broad range of globally used biodiesel fuels (22 types).

This paper summarises some comparisons between the results, referring to fuel droplet evaporation times and time evolution of droplet surface temperatures and radii, predicted by the recently developed versions of the DCM and MDQDM. The latter two models take into

account the recirculation, temperature gradient, and diffusion of species inside the droplets, based on the Effective Thermal Conductivity and Effective Diffusivity (ETC/ED) models. The main principles of the DCM and MDQDM are presented in Section 2. The results of using the DCM and MDQDM for the analysis of droplet heating and evaporation for biodiesel, diesel, gasoline and blended diesel-biodiesel fuels are presented in Sections 3 – 6, respectively. The results are summarised and final conclusions are made in Section 7.

2. Models

In the case of small components (e.g. biodiesel fuel compositions), where the number of components is relatively small, the DCM (described in [6,13]) can be facilitated. In the DCM analyses, processes inside droplets are assumed as spherically symmetric. The temperature gradient, species diffusion and internal recirculation in the liquid phase are all accounted for, using the effective thermal conductivity/effective diffusivity model [14].

The MDQDM approach is used in application to diesel, biodiesel, gasoline, and blended diesel-biodiesel fuel droplets. In this model, the actual composition of fuel is reduced to a much smaller number of representative components/quasi-components (C/QC) (see [9]). These C/QC are formed within groups of components (e.g. 9 groups of diesel fuel, 6 groups of gasoline fuel and 4 groups of fatty acid methyl ester (FAME) biodiesel fuel species), based on their thermodynamic and transport properties, chemical structures, and levels of chemical saturation. Within each group m (for biodiesel $m =$ 1 to 3, for diesel $m =$ 1 to 9, and for gasoline $m =$ 1 to 6), the new values of carbon numbers $\bar{n}_{jm}$ for QC are calculated as [9]:

$$\left.\begin{aligned}
\bar{n}_{1_m} &= \frac{\sum_{n=n_{1m}}^{n=n_{(\varphi_m+1)m}} (nX_{nm})}{\sum_{n=n_{1m}}^{n=n_{(\varphi_m+1)m}} X_{nm}}, \\
\bar{n}_{2_m} &= \frac{\sum_{n=n_{(\varphi_m+2)}}^{n=n_{(2\varphi_m+2)m}} (nX_{nm})}{\sum_{n=n_{(\varphi_m+2)}}^{n=n_{(2\varphi_m+2)m}} X_{nm}}, \\
\boldsymbol{\bar{n}_{3_m}} &= \frac{\sum_{n=n_{(2\varphi_m+3)m}}^{n=n_{(3\varphi_m+3)m}} (\boldsymbol{nX_{nm}})}{\sum_{n=n_{(2\varphi_m+3)}}^{n=n_{(3\varphi_m+3)}} \boldsymbol{X_{nm}}}, \\
&\vdots \\
\bar{n}_{l_m} &= \frac{\sum_{n=n_{((\ell-1)\varphi_m+\ell)m}}^{n=n_{k_m}} (nX_{nm})}{\sum_{n=n_{((\ell-1)\varphi_m+\ell)m}}^{n=n_{k_m}} X_{nm}},
\end{aligned}\right\} \qquad (1)$$

where n is the carbon number, $n_{1m} = n_{m(min)}$ is the minimal value of n, $n_{km} = n_{m(\max)}$ is the maximal value of n, $\ell = \text{integer}((k_m + \varphi_m)/(\varphi_m + 1))$, $\varphi_m + 1$ is equal to the number of components to be included within each quasi-component (QC) and k_m is the number of components. In contrast to [9–11], where selective fossil fuels were accounted for, in this paper, the molar fractions of quasi-components (X_{nm}) are similarly estimated but for broad types of fuels and their blends, as:

$$\left.\begin{aligned} X_{1_m} &= \sum_{n=n_{1m}}^{n=n_{(\varphi m+1)m}} X_{nm}, \\ X_{2_m} &= \sum_{n=n_{(\varphi m+2)m}}^{n=n_{(2\varphi m+2)m}} X_{nm}, \\ &\vdots \\ X_{l_m} &= \sum_{n=n_{((\ell-1)\varphi m+\ell)m}}^{n=n_{km}} X_{nm}. \end{aligned}\right\} \quad (2)$$

The studied conditions are for droplets of homogeneous temperatures and radii within the ranges of 300-360 K and 10-15 μm, respectively, moving in still air at velocities U_d= 0-35 m/s, under ambient temperatures and pressures $T_{\text{air}} = 500 - 800$ K and $p_{\text{air}} = 5 - 50$ bar, respectively.

The analysis presented in this paper is based on the 1D numerical discretisation of a spherical droplet volume into 300 concentric layers for the liquid phase. The model is a quasi-steady transient approach with time step equal to 10^{-6} seconds. The analytical solution to the transient heat conduction equation, presented in [9], is used in this paper with a number of eigenvalue terms equal to 44. Similarly, the analytical solution to the mass diffusion equation has been set with eigenvalues of 33 terms. The input parameters, grid independence check and validation, in comparison to ANSYS-Fluent predictions and experimental data, are presented in [15]. Gas properties near the droplet surface are calculated using the reference temperature $\left(T_{\text{ref}} = \frac{2}{3}T_s + \frac{1}{3}T_g\right)$. All liquid properties are calculated using the average temperature of droplets. The enthalpy of evaporation and saturated vapour pressure are calculated using the droplet surface temperature T_s. Please see [6,9], for a full description of the solution algorithm.

3. Biodiesel fuel droplets

The interest in biodiesel-diesel fuel blends has been mainly stimulated by the depletion of fossil fuels and the need to reduce emissions that contribute towards climate change [16]. Biodiesel fuel can be blended with fossil fuels at many different concentrations. For instance, a mixture of 95% diesel and 5% biodiesel (B5) fuel can be called diesel fuel, with no separate labelling required at the pump [17]. Hence, it is essential to investigate this assumption based on the estimated droplet lifetimes of diesel-biodiesel fuel blends.

In this work, the DCM has been applied to 22 types of fatty acid methyl ester (FAME) biodiesel fuels, namely, tallow (TME), lard (LME), butter (BME), coconut (CME), palm kernel (PMK), palm (PME), safflower (SFE), peanut (PTE), cottonseed (CSE), corn (CNE), sunflower (SNE), soybean (SME), rapeseed (RME), linseed (LNE), tung (TGE), hemp-oil – produced from hemp seed oil in the Ukraine (HME1), hemp-oil – produced in European Union (HME2), canola (CAN), waste cooking-oil (WCO), yellow grease oil (YME), camelina (CML), and jatropha (JME). The full composition of each of these fuels, inferred from [6,18,19], is averaged, normalised and presented in Table 1. The predicted droplet lifetimes for all 22 types of biodiesel fuel are presented in Section 6 (B100 column, Table 4).

Table 1. biodiesel fuel compositions.

FAME	C8:0	C10:0	C12:0	C14:0	C15:0	C16:0	C17:0	C18:0	C20:0	C22:0	C24:0	C16:1	C17:1	C18:1	C20:1	C22:1	C24:1	C18:2	C20:2	C18:3	C20:3	C18:4	Others
TME	-	-	0.2	2.5	-	27.9	-	23	0.4	0.4	-	2.5	-	40	0.3	0.3	-	2	-	-	-	-	0.5
LME	-	-	-	1	-	26	-	14	-	-	-	2.8	-	44	2	2	-	8	-	-	-	-	0.2
BME	5.19	2.8	3.4	10.99	-	31.66	-	10.79	0.4	0.4	-	2.4	-	26.37	1	1	-	3	-	0.6	-	-	-
CME	6	8	50	15	-	9	-	3	-	-	-	-	-	7	-	-	-	2	-	-	-	-	-
PMK	2.6	4	50	17	-	8	-	1.7	1.5	1.5	-	0.4	-	12	-	-	-	1.3	-	-	-	-	-
PME	-	-	0.26	1.29	-	45.13	-	4.47	0.35	0.17	-	0.21	-	38.39	-	-	-	9.16	-	0.19	-	-	0.38
SFE	-	-	-	-	-	5.2	-	2.2	-	-	-	-	-	76.38	-	-	-	16.22	-	-	-	-	-
PTE	-	-	-	0.5	-	8	-	4	7	7	-	1.5	-	49	-	-	-	23	-	-	-	-	-
CSE	-	-	-	2	-	19	-	2	-	-	-	-	-	31	2.5	2.5	-	41	-	-	-	-	-
CNE	-	-	-	1	-	9	-	2.5	-	-	-	1.5	-	40	1	1	-	44	-	-	-	-	-
SNE	-	-	-	-	-	5.92	-	4.15	1.38	1.38	-	-	-	18.46	-	-	-	68.41	-	0.3	-	-	-
TGE	-	-	-	-	-	3.64	-	2.55	-	13.14	-	-	-	10.1	0.81	-	-	13.75	-	51.64	-	-	4.37
HME1	-	-	-	-	-	6.62	0.21	2.06	0.45	0.25	0.23	0.33	-	11.88	0.27	0.17	0.15	56.71	-	20.67	-	-	-
SME	-	-	-	0.3	-	10.9	-	4.4	0.4	-	-	-	-	24	-	-	-	52.8	-	7.2	-	-	-
LNE	-	-	-	0.2	-	6.2	-	0.6	-	-	-	-	-	18	-	-	-	16	-	59	-	-	-
HME2	-	-	-	-	-	6.51	-	2.46	0.9	-	-	-	-	11.88	0.9	-	-	54.82	-	20.07	-	-	2.46
CAN	-	-	-	-	-	4.48	0.14	1.99	0.62	0.35	0.16	0.36	-	59.66	1.49	0.42	-	20.89	-	9.44	-	-	-
WCO	-	-	0.2	0.67	-	15.69	0.2	6.14	0.39	0.44	0.3	0.73	-	42.84	0.56	0.15	-	29.36	-	2.03	-	-	0.3
RME	-	-	-	-	-	4.93	-	1.66	0.56	-	-	-		26.61	-	22.32	0.77	24.75	-	9.7	-	-	8.7
CML	-	-	0.4	2.7	-	6.1	-	2.8	1.4	0.9	0.7	-	-	16.8	14.4	3.1	0.2	17	1.5	35.6	0.8	-	1
JTR	-	-	0.1	0.3	-	14.9	0.1	6.1	0.2	0.2	2.6	1	-	40.4	0.1	0.1	0.1	36.2	-	0.3	-	-	1.2
YGR	-	-	0.2	0.8	0.1	16.5	0.1	7.1	0.3	0.4	0.2	0.9	0.1	44.6	0.5	0.1	4.4	25.1	-	1.1	-	0.5	-

The use of the MDQDM has been applied to biodiesel fuel droplets of waste cooking oil (WCO) methyl esters, as shown in Figure 1. WCO is a typical example of biodiesel fuel with average properties and broad range of FAME components. As in [20], using the MDQDM replaces the 14 methyl esters with 5 (indicating C17.53:0, C20:0, C18:1, C18:2 and C18:3), 4 (indicating C17.613:0, C18:1, C18:2, and C18:3) and 3 (indicating C17.613:0, C18:1 and C18:2) C/QC. The initial droplet radius and temperature are 10 μm and 350 K respectively. The ambient gas temperature and pressure are 800 K and 30 bar respectively. The droplet is moving at constant velocity 10 m/s in still air.

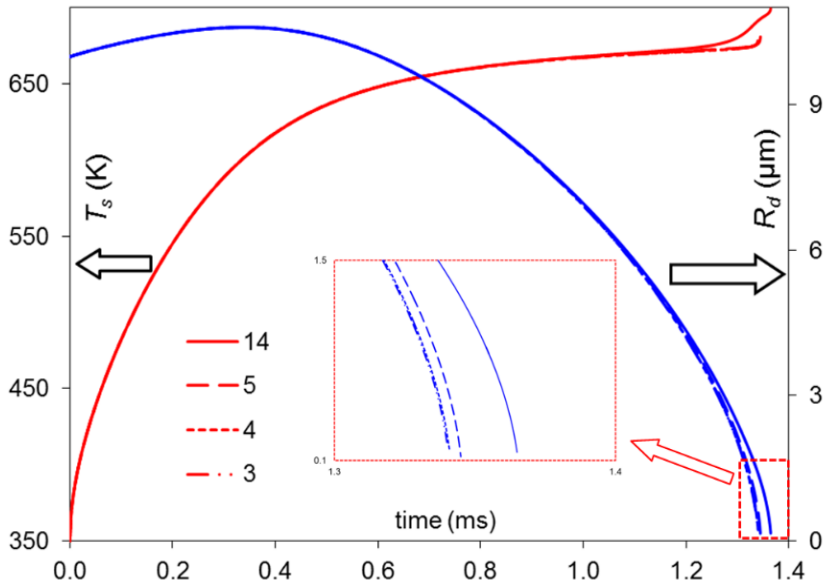

Figure 1. The plots of droplet surface temperatures (T_s) and radii (R_d) versus time for various WCO fuel using the MDQDM. The numbers of components/quasi-components 3, 4, and 5 indicate: C17.613:0, C18:1 and C18:2; C17.613:0, C18:1, C18:2, and C18:3; and C17.53:0, C20:0, C18:1, C18:2 and C18:3, respectively.

Table 2. The WCO droplet components/quasi-components (C/QC) used in the MDQDM, their CPU time, and resulted errors in predicting droplet lifetimes, in comparison to the DCM.

C/QC	FAME	CPU time (ms)	Error
14 components	See Table 1 (WCO composition)	128	-
5 C/QC	$C_{16.884}H_{33.768}O_2$ $C_{19.597}H_{39.194}O_2$ $C_{19.006}H_{36.012}O_2$ $C_{19}H_{34}O_2$ $C_{19}H_{32}O_2$	55	1.46
4 C/QC	$C_{17.705}H_{35.41}O_2$ $C_{19.006}H_{36.012}O_2$ $C_{19}H_{34}O_2$ $C_{19}H_{32}O_2$	50	1.76
3 C/QC	$C_{17.705}H_{35.41}O_2$ $C_{19.006}H_{36.012}O_2$ $C_{19}H_{34}O_2$	37	1.83

As can be seen from Figure 1, replacing the full composition of WCO methyl esters with 5, 4 and 3 C/QC produces almost identical predictions for the evolutions of T_s and R_d. The errors in predicting T_s for all (5, 4, 3) C/QC, using the MDQDM, compared to those of 14 components, using the DCM, are less than 2%. The same errors in predicting droplet lifetimes are less than 1.83%; however, using the MDQDM reduces computational time up to 96% (see Table 2).

4. Diesel fuel droplets

The diesel fuel composition used in this analysis has been inferred from [9]. The plots of typical evolutions of diesel fuel droplet surface temperatures T_s and radii R_d versus time, using the DCM and MDQDM approaches, are shown in Figure 2. The full composition of diesel fuel, combining 98 components, is considered. The droplet of 12.66 μm initial radius and 360 K temperature is moving at 10 m/s in still air of pressure and temperature equal to 32 bar and 700 K, respectively.

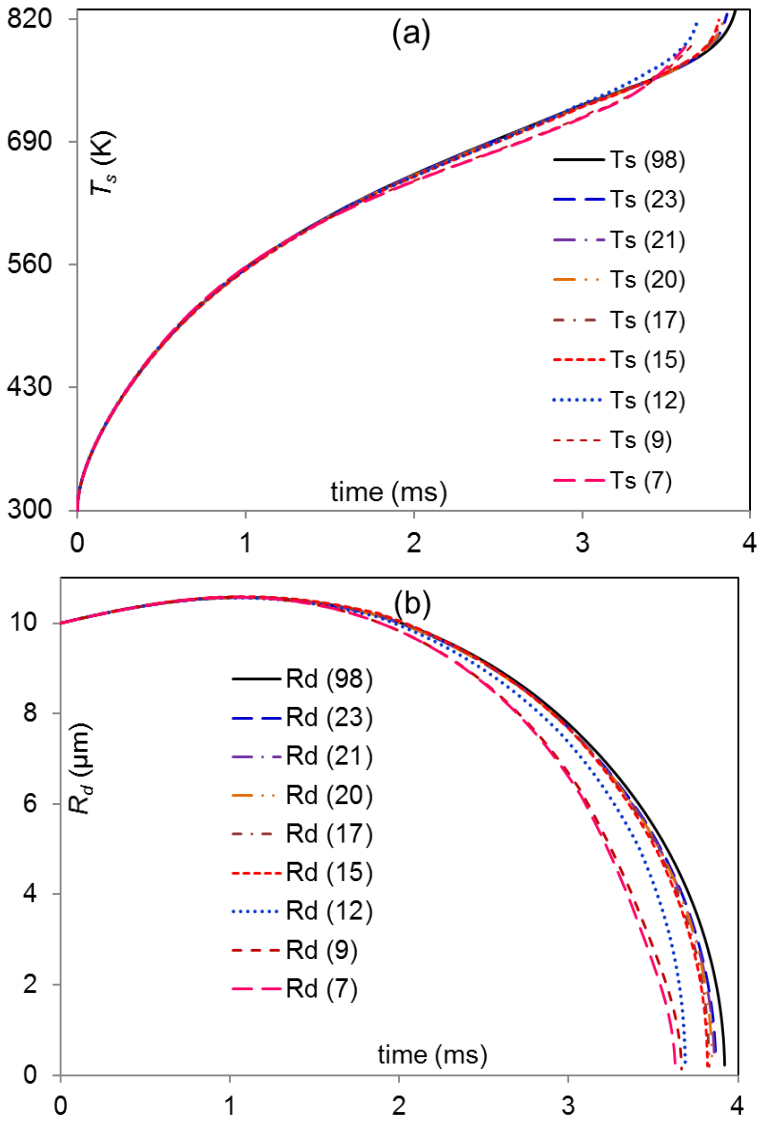

Figure 2. The plots of T_s (a) and R_d (b) versus time for a diesel fuel droplet, predicted using the MDQDM for 23, 21, 20, 17, 15, 12, 9, and 7 components/quasi-components and using the DCM for all 98 components.

As can be seen from Figure 2, nine cases have been presented. In the first case, the contributions of all 98 components are taken into account using the DCM (labelled as (98)). In the other 8 cases, the contributions of all 98 components are approximated by 23, 21, 20, 17, 15, 12, 9, and 7 C/QC using the MDQDM. One can see that the approximation of 98 components of diesel fuel by 15 C/QC leads to acceptable prediction of less than 3% error compared to the droplet lifetime predicted for 98 components, using the DCM, which can be acceptable in most applications. Similar trends are observed for other C/QC, but with slightly higher errors for less number of C/QC and less errors for higher number of C/QC.

The use of the MDQM has reduced the CPU time to its 1/6th compared with the model considering the contribution of all 98 components, as shown in Figure 3. The machine facilitated for this analysis is Intel Xeon (core duo) E8400, 2 GHz and 3 GB RAM considering 1 μs time-step.

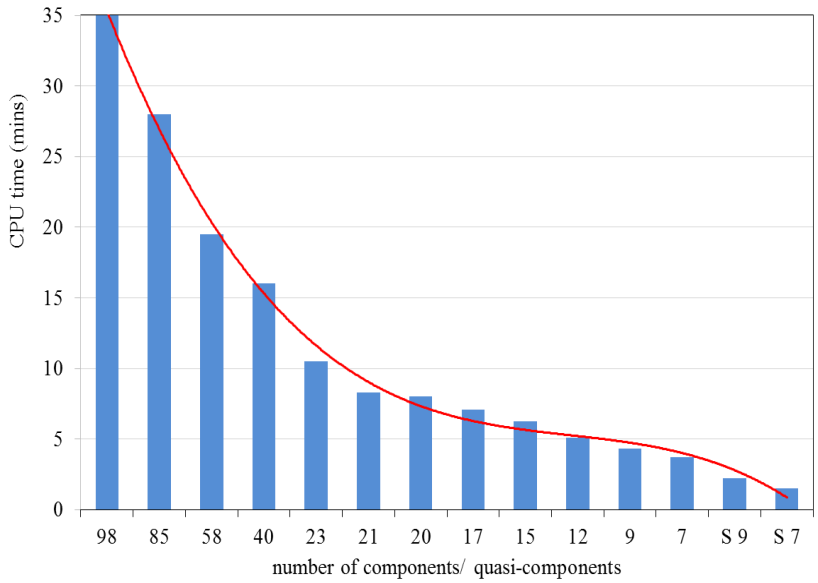

Figure 3. The plot of CPU time required for calculations of diesel fuel droplet heating and evaporation, under the same conditions as in Figure 2.

5. Gasoline fuel droplets

The evolutions of the droplet surface temperatures T_s and radii R_d versus time for gasoline FACE C (Fuel used in Advanced Combustion Engines, type C) fuel are presented in Figure 4. The droplet with initial radius 12 μm and initial temperature 300 K is assumed to be moving with velocity 20 m/s in still air. Ambient pressure and temperature are equal to 1 MPa and 550 K, respectively. The composition of gasoline FACE C is inferred from [10].

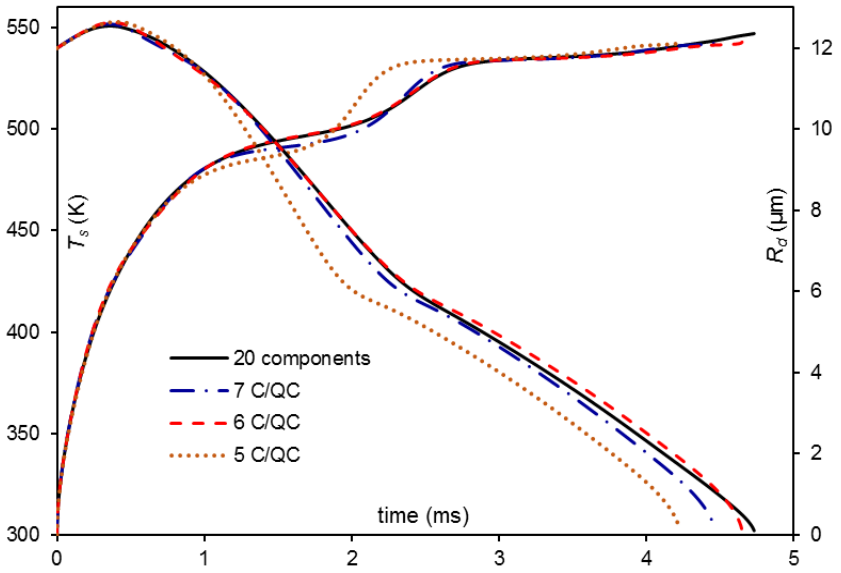

Figure 4. The plots of T_s and R_d versus time for gasoline fuel droplets, predicted using the DCM (indicated as 20 components) and MDQDM (indicated as 7, 6 and 5 components/quasi-components).

In Figure 4, four cases have been examined: (1) the contributions of all 20 components are taken into account using the DCM; (2) the contributions of 20 components are taken into account, but represented by 7 QC, $C_{5.242}H_{12.484}$, $C_{11.091}H_{24.182}$, $C_{5.274}H_{12.548}$, $C_{7.79}H_{17.58}$, $C_{10.239}H_{22.478}$, $C_{8.936}H_{11.872}$, and $C_{10.111}H_{14.222}$, using the MDQDM; (3) the contributions of 20 components are taken into account, but represented by 6 QC, $C_{5.242}H_{12.484}$, $C_{11.091}H_{24.182}$, $C_{6.181}H_{14.36}$, $C_{8.032}H_{18.064}$, $C_{8.936}H_{11.872}$, $C_{10.111}H_{14.222}$, using the MDQDM; and (4) the contributions of 20 components are taken into account, but represented by 5 QC, $C_{5.242}H_{12.484}$, $C_{11.091}H_{24.182}$, $C_{7.407}H_{16.814}$, $C_{8.936}H_{11.872}$, $C_{10.111}H_{14.222}$, using the MDQDM.

The errors in predicted droplet surface temperatures and evaporation times, using the MDQDM compared to the DCM, for 7 C/QC are less than 1% and 5.6%, respectively. The same errors predicted for 6 C/QC are less than 0.7% and 1.73%, respectively, and for 5 C/QC are less than 3.9% and 10.7%, respectively. As can be noticed from these errors, the approach of reducing 20 components of gasoline fuel to 6 C/QC gives the best results, with the smallest errors in predicted droplet temperatures and lifetimes compared to the other two approaches. These errors can be tolerated in many engineering applications. Further illustration of these modelling errors and their estimated CPU times are presented in Table 3.

Table 3. The numbers of components/quasi-components (C/QC) implemented in the MDQDM, their CPU time requirements, and droplet lifetime errors, using the same conditions as in Figure 4.

C/QC	CPU	errors
20	340	-
7	125	5.59
6	116	1.73
5	92	10.66

The use of the MDQDM can contribute to significant increase in CPU efficiency by reducing 73% of the CPU time spent to run the DCM for the same fuel. The specifications of the workstation used in this analysis are Z210, Intel core, 64-bit, 3.10 GHz and 8 GB RAM.

6. Blended diesel-biodiesel fuel droplets

As in [21], the blended fuel droplet heating and evaporation for diesel-biodiesel fuels and their blends have been investigated. Both, the DCM and MDQDM, approaches are considered – accounting for 114 components within 11 groups of hydrocarbons and methyl esters ($m =$ 1 to 3 for biodiesel fuel, and $m =$ 1 to 9 for diesel fuel (see Section 2)). As inferred from previous analyses, these models have been tested in application to blends of all 22 types of biodiesel fuel with commercially used diesel fuel (see Figure 5). In Figure 5, droplets are assumed to be moving at 10 m/s in still air, with 12.66 μm initial radius, 360 K initial temperature, and ambient pressure and temperature of 30 bar and 800 K, respectively.

Typical trends of the time evolutions of the droplet surface temperatures T_s and radii R_d of blended diesel-biodiesel fuel droplets, using the DCM, are illustrated in Figure 6 for lard (LME), waste cooking oil (WCO), tallow (TME), coconut (CME), palm (PME), rapeseed (RME), tung (TGE), and canola seed (CAN) methyl ester biodiesel fuels. In this figure, four mixtures of diesel-biodiesel fuels were shown; B100 (pure biodiesel fuel), B50 (50% biodiesel and 50% diesel fuels), B20 (20% biodiesel and 80% diesel fuels) and B5 (5% biodiesel and 95% diesel fuels). The droplet of initial radius and temperature equal to 12.66 μm and 360 K, respectively, is moving at 10 m/s in still and dry air. The air pressure and temperature are assumed as 30 bar and 800 K, respectively.

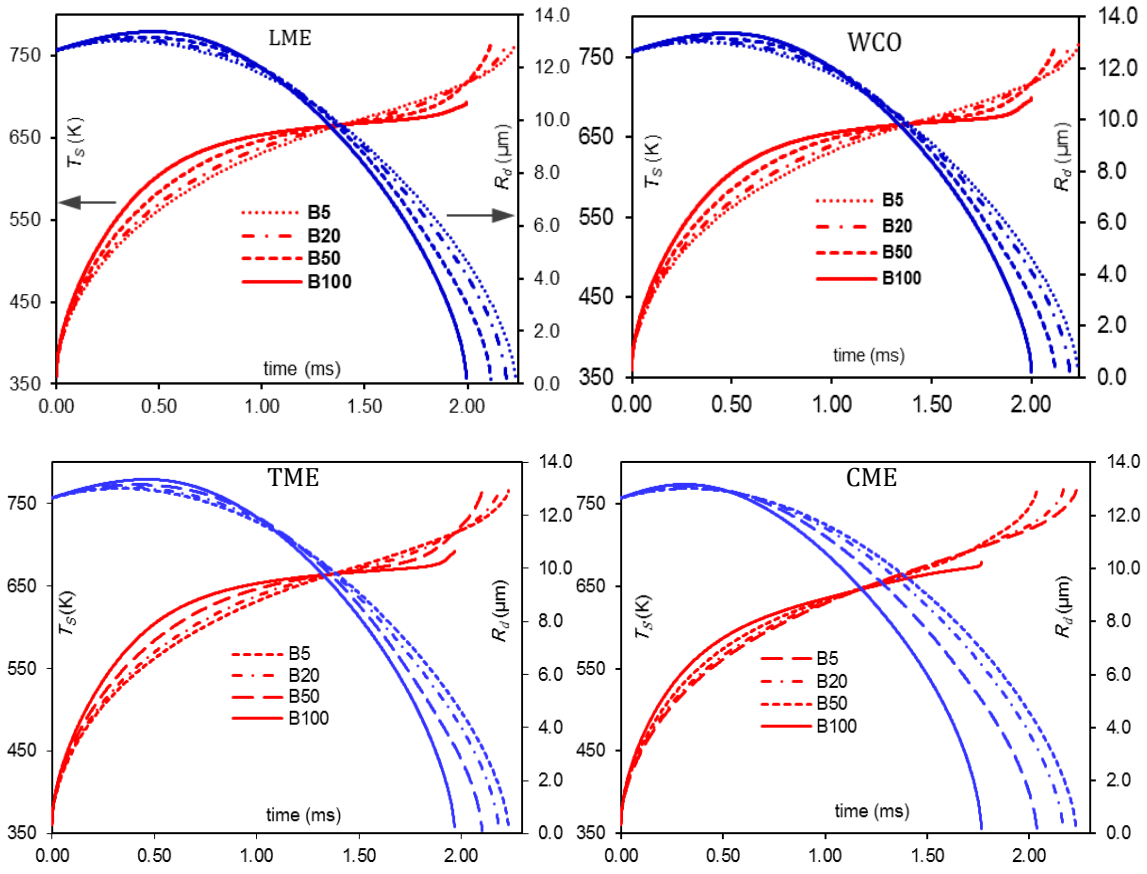

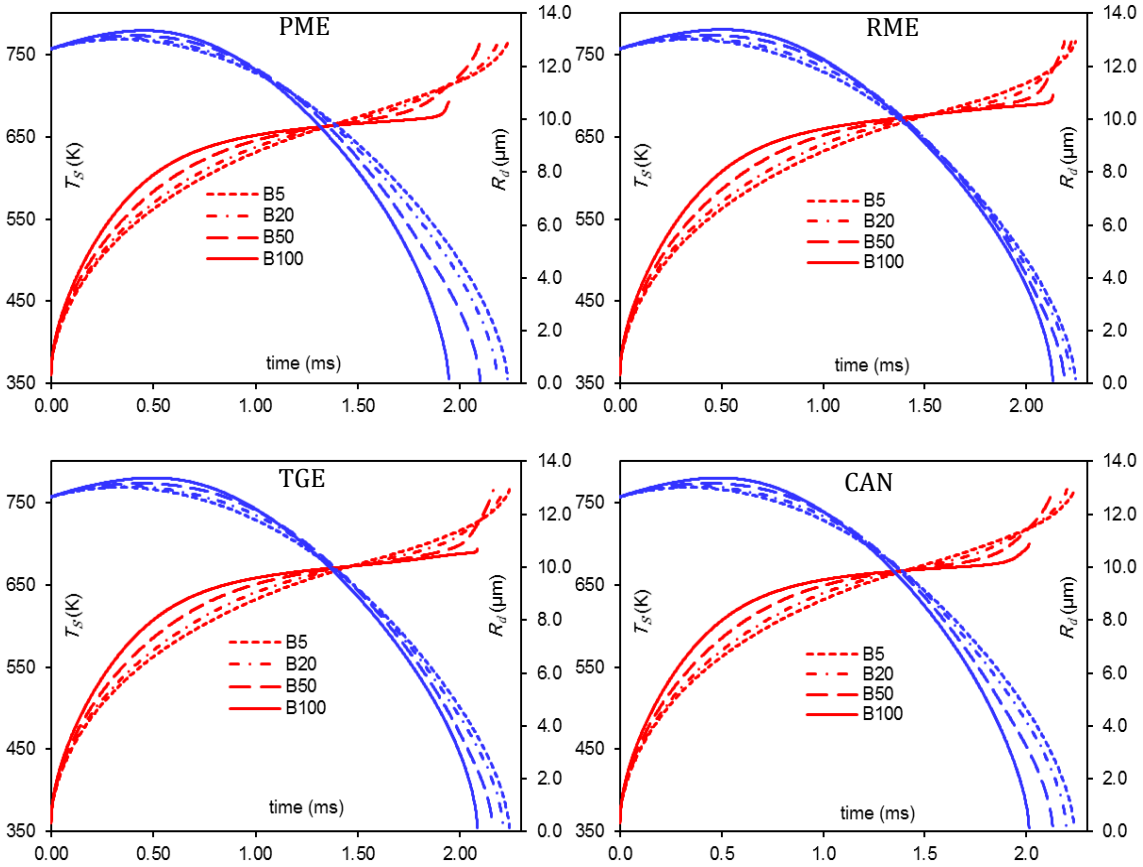

Figure 5. Droplet surface temperatures T_s and radii R_d versus time for four fractions of B5, B20, B50 and B100 fuel blends, predicted using the DCM. The following biodiesel fuels are used in these blends: LME, WCO, TME, CME, PME, RME, TGE, and CAN, as indicated on each diagram.

The estimated differences in predicted droplet lifetimes of blended diesel fuel with 22 types of biodiesel fuels are presented in Table 4. As can be seen from this table, the droplet lifetime for B100 of RME fuel is 6% less than that of diesel fuel. This reduction does not exceed 0.4% for the B5 fuel blend for the same fuel. Also, the droplet lifetime of a TGE biodiesel fuel droplet is noticeably close to that of diesel fuel droplet; it is less than 8% and 0.5% for B100 and B5 mixtures, respectively. The maximum difference in droplet lifetimes for these fuels is up to 21.6% for B100 CME, which cannot be sacrificed in any engineering application. Also, it is always lower than 5.29% for RME compared to diesel fuel one, which may be tolerated in some limited engineering applications.

Table 4. The estimated droplet lifetimes of biodiesel fuels and their diesel blends, and the differences from those of pure diesel fuel.

FAME	B100		B50		B20		B5	
	Lifetime (ms)	Diff. (%)	Lifetime (ms)	Diff. (%)	Lifetime (ms)	Diff. (%)	Lifetime (ms)	Diff. (%)
TME	1.967	12.6	2.102	6.6	2.184	2.9	2.232	0.80
LME	1.995	11.3	2.114	6.0	2.190	2.7	2.234	0.71
BME	1.943	13.6	2.089	7.2	2.180	3.1	2.232	0.80
CME	1.765	21.6	2.036	9.5	2.166	3.7	2.229	0.93
PMK	1.846	18.0	2.050	8.9	2.169	3.6	2.230	0.89
PME	1.944	13.6	2.097	6.8	2.183	3.0	2.232	0.80
SFE	1.980	12.0	2.122	5.7	2.195	2.4	2.235	0.67

PTE	2.052	8.8	2.138	5.0	2.199	2.3	2.236	0.62
CSE	2.014	10.5	2.128	5.4	2.197	2.4	2.236	0.62
CNE	2.002	11.0	2.128	5.4	2.197	2.4	2.236	0.62
SNE	2.011	10.6	2.132	5.2	2.200	2.2	2.237	0.58
SME	1.981	12.0	2.127	5.5	2.198	2.3	2.236	0.62
RME	2.131	5.3	2.188	2.8	2.222	1.2	2.242	0.36
LNE	1.991	11.5	2.141	4.8	2.206	2.0	2.239	0.49
TGE	2.085	7.3	2.160	4.0	2.211	1.7	2.240	0.44
HME1	2.022	10.1	2.138	5.0	2.203	2.1	2.237	0.58
HME2	1.994	11.4	2.135	5.1	2.202	2.1	2.238	0.53
CAN	2.014	10.5	2.130	5.3	2.199	2.3	2.236	0.62
WCO	2.002	11.0	2.121	5.7	2.194	2.5	2.235	0.67
CML	2.064	8.3	2.153	4.3	2.209	1.8	2.239	0.49
JTR	2.047	9.0	2.133	5.2	2.198	2.3	2.236	0.62
YGR	2.077	7.7	2.149	4.5	2.203	2.1	2.237	0.58

A typical example of the evolutions of T_s and R_d over time for a B5 diesel-biodiesel fuel blend (5% biodiesel and 95% diesel) droplet is shown in Figure 6. The droplet parameters are taken as equal to the ones used in Figure 5. The ambient air (gas) pressure and temperature are assumed to be equal to 32 bar and 700 K, respectively.

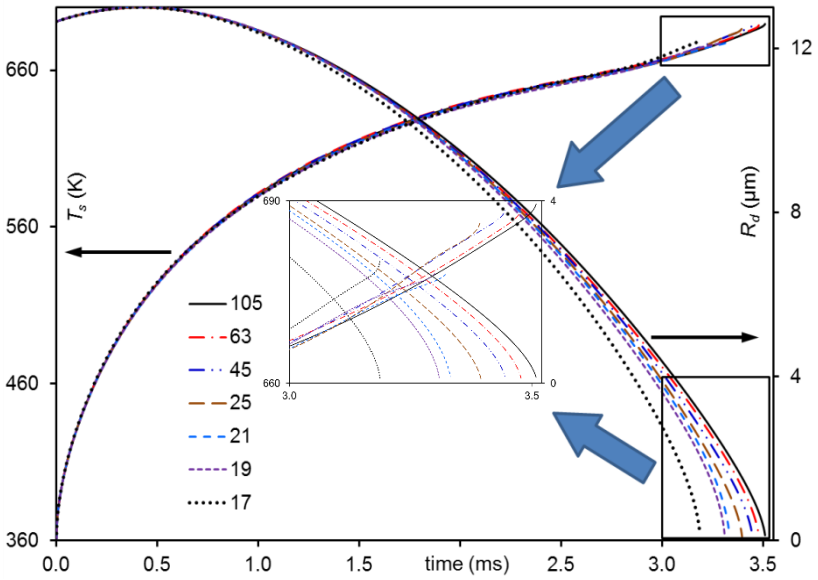

Figure 6. The plots of T_s and R_d versus time for various B5 diesel/SME blend, using the DCM and MDQDM approaches.

As can be seen from Figure 6, the approximations of the blended fuel of 105 hydrocarbons and methyl esters with 25 C/QC lead to an underestimation of the droplet lifetime by less than 3.2%. This underestimation increases to a range of 4%-4.5% for a selection range between 21 to 17 C/QC, respectively. The errors in predicted droplet surface temperatures for all MDQDM approximations were up to 2%. Using the MDQDM for this analysis has made significant contribution to the CPU efficiency of the code. An example of the impact of using the MDQDM approach on the computational costs among these several approximations is illustrated in Figure 7.

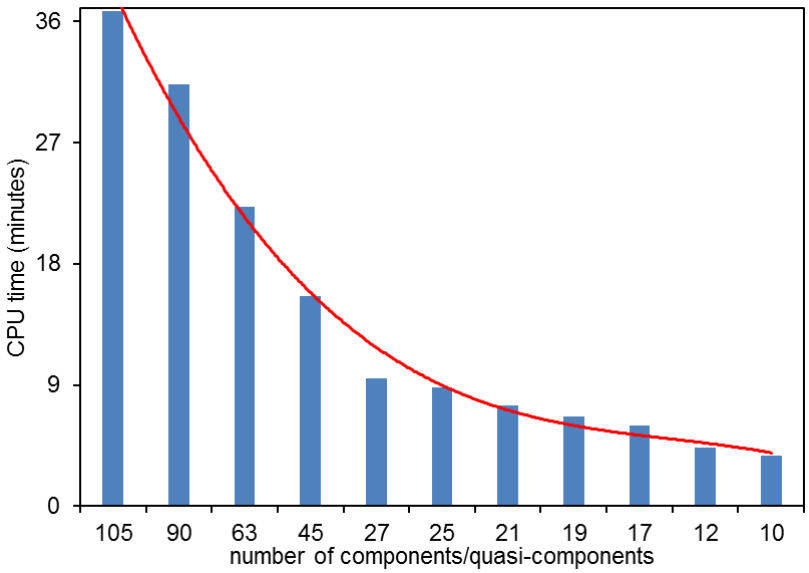

Figure 7. The plot of CPU time required for calculations of droplet heating and evaporation versus the number of components/quasi-components for B50 diesel/SME fuel droplets, using the same conditions as in Figure 6.

As can be seen from Figure 7, approximating 105 components of the B50 blend of diesel/SME fuels with 17 C/QC reduces the required CPU time by more than 83%, compared with the DCM approach, considering the contributions of all 105 components. Also, the droplet lifetimes predicted for the 17 C/QC of B50 and B5 blends are, respectively, 4% and 9% less than those predicted by the DCM for the same blends. Such an option can ensure a good compromise between CPU efficiency of the model and its accuracy when small errors in predicted droplet evaporation times can be tolerated for commonly used fuel blends. The specifications of the workstation used in this analysis are Z210, Intel core, 64-bit, 3.10 GHz and 8 GB RAM.

As can be seen from all results, T_s exceeds the average critical temperatures of these fuels. However, due to diffusion of species inside droplets, the heaviest components with high critical temperatures (potentially well above the average critical temperature of dominant components at initial time) become the dominant ones near the evaporation time (see Figure 8). For example, T_c (Heptacosane, $C_{27}H_{54}$) = 1000.84 K, which is well above the maximum temperature of diesel fuel (820 K, Figure 2).

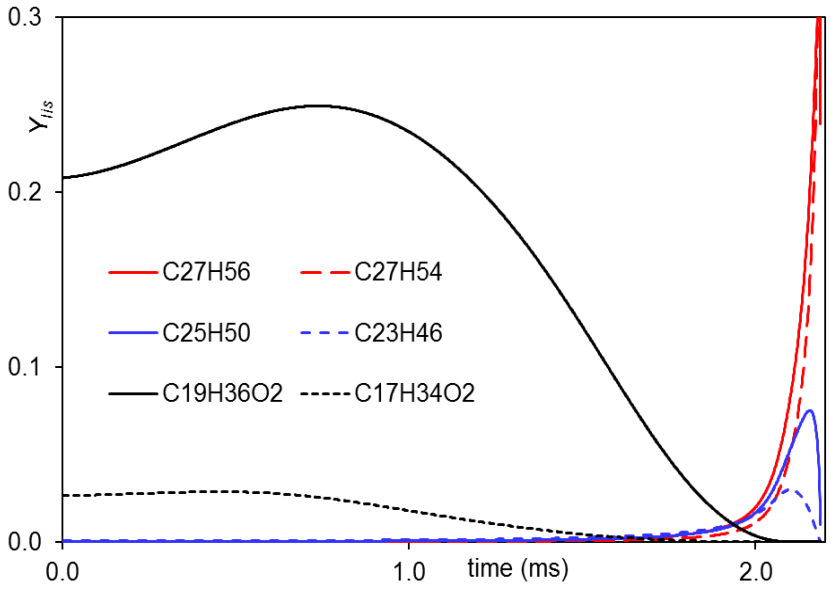

Figure 8. Liquid mass fractions at the droplet surface (Y_{lis}) versus time for 6 representative components of B50 fuel mixture. The red coloured curves refer to alkanes, the blue curves refer to cycloalkanes, and the black curves refer to FAME.

7. Conclusions

The modelling of the heating and evaporation of multi-component biodiesel, diesel, gasoline, and blended diesel-biodiesel fuel droplets has been performed using the Discrete Component model (DCM) and the Multi-Dimensional Quasi-Discrete Model (MDQDM). In both models, the full fuel compositions, effects of species diffusion, temperature gradient and recirculation inside droplets are accounted for.

It has been demonstrated that replacing the full composition of biodiesel fuels (14 FAME components in the case of WCO) with 5, 4 and 3 C/QC, using the MDQDM, leads to negligible errors in predicting droplet surface temperatures (less than 2%) and evaporation times (less than 1.83%), compared to the predictions of the DCM. Also, using the MDQDM can reduce computational time up to its 0.04^{th}.

In the case of diesel fuel, using the MDQDM leads to less than 3% error in predicted droplet lifetime, compared to that of the DCM, which can be acceptable in most applications. This approach can reduce the CPU time to its $1/6^{th}$ compared with the DCM, considering the contributions of all 98 components.

Similarly, replacing the full composition of FACE C gasoline fuel (20 hydrocarbons) with 6 C/QC, using the MDQDM, has led to less than 1.73% error in predicted droplet lifetime. This approach can contribute to reducing CPU time with up to 73% compared to that spent using the DCM.

The influence of increasing the fraction of biodiesel in the diesel-biodiesel mixture on droplet surface temperature and evaporation time is shown to be noticeable, and it needs to be accounted for in engineering modelling. Smaller fractions of biodiesel fuel (up to 5%) have very small effects on the evolutions of droplet surface temperatures (T_s) and radii (R_d). However, the maximum difference in droplet lifetimes for these fuels is up to 21.6% for B100 CME, which cannot be sacrificed in any engineering application.

Acknowledgment

The author is grateful to S.S. Sazhin of the University of Brighton and N. Al-Esawi of Coventry University for useful discussions, and the Centre for Mobility and Transport – Coventry University for providing financial support to work on this project.

References

[1] S.S. Sazhin, Advanced models of fuel droplet heating and evaporation, Prog. Energy Combust. Sci. 32 (2006) 162–214. doi:10.1016/j.pecs.2005.11.001.
[2] Y. Ra, R.D. Reitz, A vaporization model for discrete multi-component fuel sprays, Int. J. Multiph. Flow. 35 (2009) 101–117. doi:10.1016/j.ijmultiphaseflow.2008.10.006.
[3] S. Tonini, G.E. Cossali, A multi-component drop evaporation model based on analytical solution of Stefan–Maxwell equations, Int. J. Heat Mass Transf. 92 (2016) 184–189. doi:10.1016/j.ijheatmasstransfer.2015.08.014.
[4] M. Al Qubeissi, S.S. Sazhin, Models for droplet heating and evaporation: an application to biodiesel, diesel and gasoline fuels, Int. J. Eng. Syst. Model. Simul. 9 (2017) 32. doi:10.1504/IJESMS.2017.10002565.
[5] A. Arabkhalaj, A. Azimi, H. Ghassemi, R. Shahsavan Markadeh, A fully transient approach on evaporation of multi-component droplets, Appl. Therm. Eng. 125 (2017) 584–595. doi:10.1016/j.applthermaleng.2017.07.054.
[6] S.S. Sazhin, M. Al Qubeissi, R. Kolodnytska, A.E. Elwardany, R. Nasiri, M.R. Heikal, Modelling of biodiesel fuel droplet heating and evaporation, Fuel. 115 (2014) 559–572. doi:10.1016/j.fuel.2013.07.031.
[7] M. Al Qubeissi, Heating and evaporation of multi-component fuel droplets, WiSa, Stuttgart, Germany, 2015.
[8] S.S. Sazhin, Modelling of fuel droplet heating and evaporation: Recent results and unsolved problems, Fuel. 196 (2017) 69–101. doi:10.1016/j.fuel.2017.01.048.
[9] S.S. Sazhin, M. Al Qubeissi, R. Nasiri, V.M. Gun'ko, A.E. Elwardany, F. Lemoine, F. Grisch, M.R. Heikal, A multi-dimensional quasi-discrete model for the analysis of Diesel fuel droplet heating and evaporation, Fuel. 129 (2014) 238–266. doi:10.1016/j.fuel.2014.03.028.
[10] M. Al Qubeissi, S.S. Sazhin, J. Turner, S. Begg, C. Crua, M.R. Heikal, Modelling of gasoline fuel droplets heating and evaporation, Fuel. 159 (2015) 373–384. doi:10.1016/j.fuel.2015.06.028.
[11] M. Al Qubeissi, S.S. Sazhin, G. de Sercey, C. Crua, Multi-dimensional quasi-discrete model for the investigation of heating and evaporation of Diesel fuel droplets, in: 26th Eur. Conf. Liq. At. Spray Syst., University of Bremen, Bremen, Germany, 2014. CD.
[12] M. Al Qubeissi, S.S. Sazhin, A.E. Elwardany, Modelling of blended Diesel and biodiesel fuel droplet heating and evaporation, Fuel. 187 (2017) 349–355. doi:10.1016/j.fuel.2016.09.060.
[13] M. Al Qubeissi, R. Kolodnytska, S.S. Sazhin, Biodiesel fuel droplets: modelling of heating and evaporation processes, in: 25th Eur. Conf. Liq. At. Spray Syst., Crete, Greece, 2013.
[14] B. Abramzon, W.A. Sirignano, Droplet vaporization model for spray combustion calculations, Int. J. Heat Mass Transf. 32 (1989) 1605–1618. doi:10.1016/0017-9310(89)90043-4.
[15] O. Rybdylova, M.A. Qubeissi, M. Braun, C. Crua, J. Manin, L.M. Pickett, G. de Sercey, E.M. Sazhina, S.S. Sazhin, M. Heikal, A model for droplet heating and its implementation into ANSYS Fluent, Int. Commun. Heat Mass Transf. (2016). doi:10.1016/j.icheatmasstransfer.2016.05.032.
[16] M. Lapuerta, O. Armas, J. Rodriguezfernandez, Effect of biodiesel fuels on diesel engine emissions, Prog. Energy Combust. Sci. 34 (2008) 198–223. doi:10.1016/j.pecs.2007.07.001.
[17] US Department of Energy: Energy Efficiency and Renewable Energy, Alternative Fuels Data Centre, (n.d.). http://www.afdc.energy.gov (accessed June 23, 2017).

[18] S.K. Hoekman, A. Broch, C. Robbins, E. Ceniceros, M. Natarajan, Review of biodiesel composition, properties, and specifications, Renew. Sustain. Energy Rev. 16 (2012) 143–169. doi:10.1016/j.rser.2011.07.143.
[19] M. Al Qubeissi, S.S. Sazhin, C. Crua, J. Turner, M.R. Heikal, Modelling of biodiesel fuel droplet heating and evaporation: effects of fuel composition, Fuel. 154 (2015) 308–318. doi:10.1016/j.fuel.2015.03.051.
[20] M. Al Qubeissi, S.S. Sazhin, Blended biodiesel/Diesel fuel droplet heating and evaporation, in: 27th Eur. Conf. Liq. At. Spray Syst., Brighton, UK, 2016: p. 179. https://www.conference-service.com/ILASS2016/documents/ILASS%202016%20programme.pdf.
[21] M. Al Qubeissi, S.S. Sazhin, A.E. Elwardany, Modelling of blended Diesel and biodiesel fuel droplet heating and evaporation, Fuel. 187 (2017) 349–355. doi:10.1016/j.fuel.2016.09.060.